Chemical Engineering Journal 103 (2004) 123–131

Chemical Engineering Journal

www.elsevier.com/locate/cej

Influence of structural properties of alum and ferric flocs on sludge dewaterability

Christelle Turchiuli*, Claire Fargues

Département Génie Industriel Alimentaire, UMR Cemagref, INRA, INAPG, ENSIA, 1 Avenue des Olympiades, 91744 Massy Cedex, France

Received 19 January 2004; received in revised form 5 May 2004; accepted 6 May 2004

Abstract

Sludges are made of flocs produced during the coagulation stage. Their dewatering not only depends on the equipment used but also on the chemical, structural and physical characteristics of flocs. In this study, the relation between floc structure and sludge dewaterability is investigated beside the influence of the operating conditions during coagulation. Eight synthetic clay flocs families are produced using clay suspensions with four initial solids concentrations ranging from 0.5 to 5 g L^{-1} and two coagulants ($Al_2(SO_4)_3$ and $FeCl_3$). Flocs structure is characterised by their fractal dimension and by the size of the basic units (clusters, aggregates) they are made from. Fractal dimension values about 2.5 are indicative of rather compact structures with slightly looser flocs obtained when using $FeCl_3$. Except for clusters, larger in ferric flocs, the basic units sizes are similar whatever the coagulant used and they decrease when the solids concentration during coagulation is increased. Sludge dewaterability is estimated from the bound water content and the capillary suction time (CST) giving respectively information on the extent and on the rate of water removal. Ferric flocs contain about 20% less bound water but exhibit higher CST values and therefore higher resistance to water removal than alum ones. Flocs structure and sludge dewaterability are found linked. The sludge bound water content is found to decrease with the floc fractal dimension: less compact flocs contain more water but less bound water. And the capillary suction time is lower when sludges are made of smaller flocs.

Keywords: Alum sludge; Ferric sludge; Dewatering; Fractal dimension; Floc structure; Bound water; Capillary suction time

1. Introduction

Sludge produced in water plants consists of bulk water together with a floc phase produced during the coagulation stage. The removal of water from sludge in dewatering units depends on the chemical, structural and physical (size, density) characteristics of flocs [1–3].

Flocs are made from complex arrangements of solids particles, hydroxide precipitates and water taken in during their growth. As shown in Fig. 1, they have irregular shapes and rather loose structures thought to be made up of three basic units corresponding to three size scales [4]. In this three-tiered particle structure notation, primary particles are supposed to group into clusters (level 1) containing dry solids and associated bound water. Aggregates (level 2) are produced by association of these clusters along with internal water, retained between clusters as part of the floc structure. Under low shear rates, aggregates form large-size flocs (level 3) through loose associations. Whilst flocs have low shear strength and are easily ruptured by external forces, aggregates and clusters are characterised by significant shear strengths. During mechanical sludge dewatering, the degree of floc breakage and deformation affecting the performances of the process therefore not only depends on the equipment used but also on the floc structure which has to be considered beside the traditional dewaterability indices for dewatering process optimisation.

1.1. Floc structure characterisation

The flocs structure can be described by the size of the different basic units and by the volume floc fractal dimension D_3. Actually, fractal theory has been successfully used to explain the decrease of floc density with floc size [5,6]. According to Mandelbrot [7], the number n of primary particles of diameter d_0 contained in a fractal floc of size d follows the power-law relation:

$$n = k\left(\frac{d}{d_0}\right)^{D_3} \quad (1)$$

* Corresponding author. Tel.: +33 1 6993 5093; fax: +33 1 6993 5044.
E-mail address: turchiuli@ensia.fr (C. Turchiuli).

1385-8947/$ – see front matter © 2004 Elsevier B.V. All rights reserved.
doi:10.1016/j.cej.2004.05.013

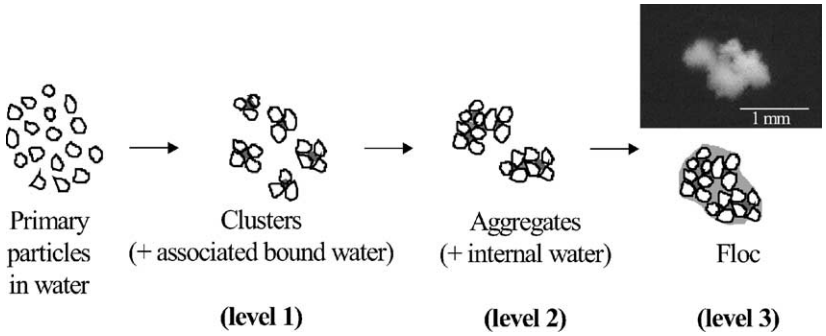

Fig. 1. The three basic units of sludge floc structure.

Therefore, assuming that flocs are spherical and made of n primary particles and water, the floc density ρ_{floc} is given by

$$\rho_{\text{floc}} = \frac{m_{\text{particle}} + m_{\text{water}}}{V_{\text{floc}}} = \frac{\rho_s n(\pi d_0^3/6) + \rho_w[(\pi d^3/6) - n(\pi d_0^3/6)]}{\pi d^3/6}$$

leading to

$$\rho_{\text{floc}} = \rho_w + k\left(\frac{d}{d_0}\right)^{D_3-3}(\rho_s - \rho_w) \quad (2)$$

where ρ_s and ρ_w are, respectively, the density of the primary particles and water. A fractal dimension D_3 smaller than the Euclidean dimension 3 indicates an open structure with density decreasing with size d.

1.2. Dewaterability indices

To characterise sludge dewaterability, capillary suction time (CST) is among the most commonly used indices for filtering techniques. It provides an empirical measure of the resistance offered by the sludge to the withdrawal of water and is a good indicator of the rate of dewatering (the lower the CST the higher the dewatering rate). Dewaterability can also be characterised by the sludge bound water content as it represents the not easily removable fraction of sludge water and will be an indicator of the extent of dewatering. Actually, the removal of sludge water is a solid/liquid separation requiring the forces binding the liquid to the solids to be overcome. Due to the complex structure of sludge flocs, it is agreed that there are four types of water in sludges [8,9]:

- *Bulk water*: surrounds sludge flocs but is not related to the solids. Represents the largest part of the sludge and can be eliminated by the application of weak mechanical strains. Thermodynamically, it behaves as pure water.
- *Interstitial water*: trapped within the floc structure or held by capillary forces between particles. Becomes bulk water when flocs units are broken. Removed by classical mechanical dewatering devices.
- *Surface water*: associated with individual particles by adsorption or absorption. It cannot be removed by purely mechanical means.
- *Chemically bound water*: fixed to the solids by strong chemical bindings. Is released only by thermal drying at temperatures above 105 °C.

To simplify, the aqueous part of sludge that behaves like pure water is generally called *free* water while the other part, which, due to significant binding to the solids has different properties from those of pure water, is called *bound* water. For good dewatering performances, it must be as low as possible.

The aim of this study was to investigate how chemical conditioning of clay suspensions can modify the structure and dewaterability of flocs. Synthetic sludges were prepared by metal ion coagulation of aqueous clay particles suspensions with different solids concentrations using ferric chloride or aluminium sulphate. The floc structure was described by estimating both the size of the basic units constituting flocs and the floc volume fractal dimension D_3. Basic units size was evaluated performing particle size measurements at different stages of the coagulation–flocculation process. Flocs size, fractal dimension and density were estimated by analysing images of flocs under settling [10]. It was followed by dewaterability tests measuring the bound water content of the sludges and their capillary suction time. Primary emphasis was placed on the response of these floc properties to the varied initial clay suspension concentrations and the different coagulants. From these results, the impact of the flocs structural properties on the sludge dewaterability was investigated. Correlations between conditions of coagulation, flocs properties and resulting sludges dewaterability were sought in order to deduce rules for the choice of conditions for coagulation leading to the best sludge dewaterability.

2. Experimental

2.1. Synthetic sludges

Synthetic sludges were prepared in a laboratory jar test apparatus (Floclab, Prolabo, F) by metal ion coagulation of

aqueous clay suspensions of various concentrations made from a commercial clay paste diluted in tap water (pH ∼ 7.2; hardness ∼19 °F; initial turbidity = 0.27 NTU (Hach turbidimeter no. 2100)). The median diameter of the initial clay particles was about 4 μm (laser diffraction) and their density measured as 2015 kg m^{-3} (Le Chatelier Candelot volume-meter). Experiments were conducted at room temperature (21 °C) in 1 l beakers. Two commonly used coagulants were tested: aluminium sulphate ($Al_2(SO_4)_3{\cdot}14H_2O$, Aventis, F) and ferric chloride ($FeCl_3$, Produits Chimiques de Loos, F). In both cases, an anionic copolymer of acrylamide and acrylic acid was used as flocculant aid (Prosedim ASP 25; Degrémont Erpac, F). The paddle rotation speed of the flocculator was set at 200 rpm and, when necessary, the pH was adjusted to 7 using 1 M NaOH prior to adding the coagulant. After 1.5 min, the flocculant was added and after three more minutes the rotation speed was lowered to 40 rpm during 17 min to allow the flocs to grow. Whilst for the flocs characterisation, slow mixing was maintained in the beaker until they were sampled and analysed, for sludge characterisation, the paddle rotation was stopped allowing flocs to settle at the bottom of the beaker.

The amounts of coagulant and flocculant added were optimised for each initial clay concentration and coagulant using minimum residual turbidity of the supernatant after 10 min settling as criteria (<5 NTU). Results of the coagulation/flocculation optimisation tests for the eight clay aggregates families investigated are summarised in Table 1. Despite the metallic ions concentrations [M^{3+}] (with M = Al or Fe) were different it was checked that in any case, the same coagulation mechanism occurred. Actually, as shown on Fe(III) and alum coagulation diagrams given in Fig. 2 [11], all the points corresponding to the conditions of Table 1 are in the sweep coagulation zone where coagulation is due to the enmeshment of the colloid particles within hydroxide precipitates ($Al(OH)_3$ or $Fe(OH)_3$).

2.2. Fractal dimension analysis

By including Eq. (1) in the force-balance achieved on a settling particle, an expression of the floc terminal velocity u_l can be obtained taking the floc diameter d and the fractal dimension D_3 into account. In the case of porous and non-spherical flocs, the difficulty is to choose a relationship to express the drag force. It has been checked in a previous work [10] that the model clay flocs studied here, settling in intermediate range, could be considered as impermeable due to their rather high D_3 values (greater than 2, the lowest limit above which flocs can be considered as impermeable [12]). Assuming a degree of true sphericity Ψ of 0.6 [5,10] an expression of the drag coefficient C_D was obtained [13]:

$$C_D = 43.7\,Re_p^{-0.596} \quad (3)$$

leading to the following expression for u_l:

$$u_l = B \cdot d^{(D_3-1.4)/1.4} \quad (4)$$

where B is a constant for a given family. Fractal dimension D_3 of the flocs can therefore be determined from the log–log plot of their settling rates u_l versus their diameters d. The free settling test is a widely used method for the determination of u_l and d values of fractal particles [5,12,14]. In this study, free settling tests were performed in a quiescent settling column (height = 600 mm; diameter = 50 mm) filled with tap water at room temperature and immersed in a square water bath to eliminate optical distorsion. The settling of the flocs gently sampled with a wide mouth pipette in the beaker immediately after the flocculation step was

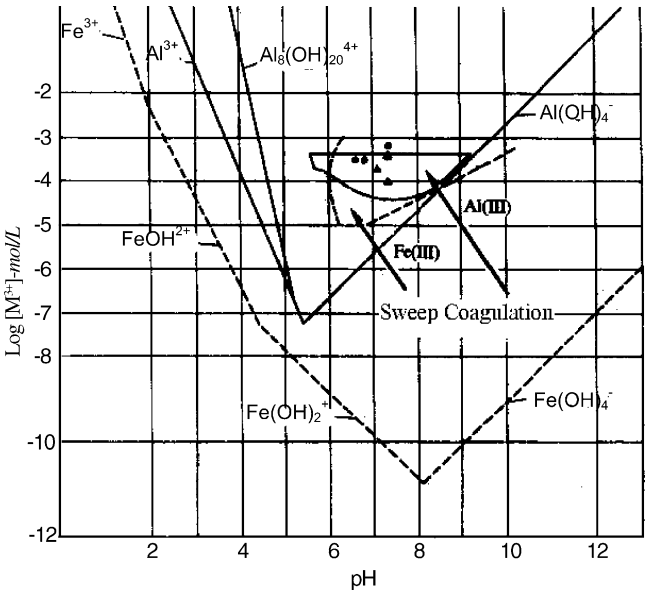

Fig. 2. Fe(III) and alum coagulation diagrams—sweep coagulation zone [11]: (●) $FeCl_3$ and (▲) $Al_2(SO_4)_3{\cdot}14H_2O$.

Table 1
Results of the coagulation/flocculation optimisation tests (M^{3+} = Fe^{3+} or Al^{3+}; Θ ∼ 20 °C; pH ∼ 7; C_{Fe} = 571 g L^{-1}; C_{Al} = 645.6 g L^{-1}; $C_{flocculant}$ = 0.1 g L^{-1})

Coagulant	$FeCl_3$				$Al_2(SO_4)_3{\cdot}14H_2O$			
C_{solids} (g L^{-1})	0.5	1	2	5	0.5	1	2	5
$V_{coagulant}$ (×10^{-6} L)	85	85	130	180	50	85	100	250
[M^{3+}] (×10^{-3} g L^{-1})	16.7	16.7	25.5	35.3	2.9	5.0	5.9	14.7
[M^{3+}]/C_{solids} (×10^{-3})	33.4	16.7	12.75	7.06	5.8	5.0	2.95	2.94
$V_{flocculant}$ (×10^{-3} L)	1	1.8	1.8	2.2	1	1	1	2
Turbidity (NTU)	1.8	1.8	2.4	4	1.5	1.7	1.9	4.4

observed using a CCD camera (Cohu 4912-5000) equipped with a macrolens (magnification 30×, 8 mm × 5 mm field of observation) and connected to a video recorder. The focusing plane was situated near the column axis and at a depth of 20 cm below the release point to ensure that the recorded flocs had reached their terminal velocity. Due to the large diameter of the column hydrodynamic interactions with the walls could be neglected. The replayed tapes were analysed with NIH 1.60 (Scion Corporation, USA). The floc diameter d was approximated by the apparent projected area diameter $D_{app} = \sqrt{4A/\pi}$ (with A = projected area of the particle). For each experimental condition about 200 flocs (from at least four coagulation/flocculation and settling procedures) were analysed and all the data were averaged from 3 to 15 images per floc (depending on the settling rate).

2.3. Basic units size measurements

Particle size analyses were performed on samples picked-up from the beaker at different stages of the coagulation–flocculation process using a Malvern-Microsizer laser diffraction instrument. Samples to be analysed were introduced into the 450 mL sampling beaker containing demineralized water where a stirrer allowed keeping the particles in suspension and a volumetric pump provided circulation of the sample through the analysis cell. Due to the relatively low strength of flocs, forces generated by the stirring device and the pump ruptured them. But it was checked that aggregates and clusters were preserved when the rotation speed of the stirrer was set below 1000 rpm since no primary particle appeared in the mono-modal particle size distributions obtained. Samples were analysed in the standard poly-dispersed mode using Mie theory.

2.4. Dewaterability tests

2.4.1. Capillary suction time

At the end of the coagulation step, flocs were let to settle and the supernatant was removed to obtain a 5% (w/w) clay concentration. 5 mL samples of this sludge were gently picked-up and their capillary suction time was measured at room temperature with a CST apparatus type 130 (Triton, GB) using Whatman no. 17 chromatography grade paper with the rougher side uppermost. Each measurement was repeated three times and for each operating condition two series of flocs obtained separately were analysed.

2.4.2. Bound water content

Clay flocs suspensions remaining at the bottom of the beaker after 30 min of settling and elimination of the supernatant were placed in the funnel of a standard Büchner apparatus equipped with a Whatman GF/C filtering medium. A vacuum of about 680 mmHg was applied for 45 min and the filter cake obtained was divided into two samples for the sludge total and bound water contents determination.

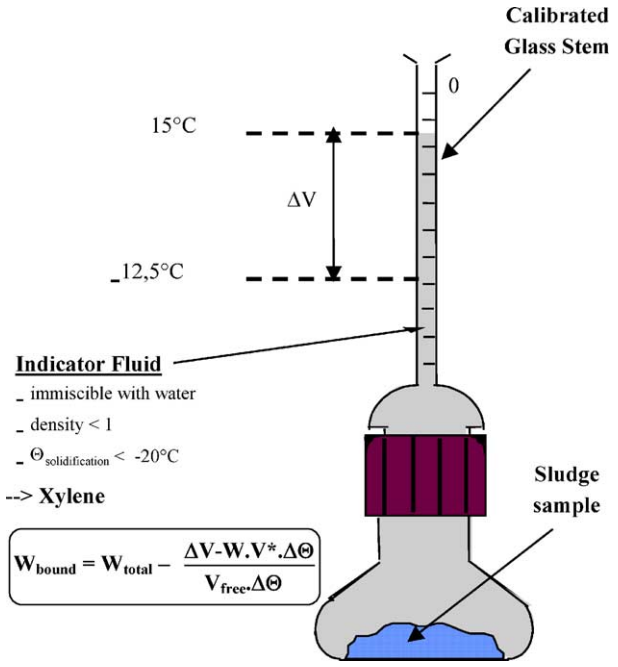

Fig. 3. Measurement of the bound water content using the dilatometric method. W_{total}: total water content of the sludge sample (kg); W: weight of indicator fluid (kg); V^*: coefficient of volume expansion of indicator fluid (1.098×10^{-3} L kg^{-1} °C^{-1}); V_{free}: coefficient of volume expansion of free water (3.83×10^{-3} L kg^{-1} °C^{-1}); $\Delta\Theta$: temperature decrease causing the volume variation ΔV.

The total water content was determined by drying at 105 °C until a constant weight was reached. The bound water content was measured using the dilatometric method [15]. It is based on the assumption that free water freezes at temperatures near the freezing point of pure water whereas bound water does not freeze even at temperatures as low as −20 °C. The volume expansion observed when cooling sludge to temperatures down to −20 °C is therefore solely due to the water–ice transformation of the free water. Its measurement allows the determination of both the free water content and the bound water content of the sample knowing its total water content (Fig. 3). Volume expansion measurements were performed using xylene as an indicator fluid between room temperature and –12.5 °C. It was checked that no further volume variation due to the water transformation occurred for temperatures down to −20 °C.

3. Results and discussion

3.1. Flocs characteristics

Fig. 4 gives the evolution of the median volume diameter d_{50} measured as a function of the time during the coagulation step. All the curves obtained are rather similar in shape with two main parts. The first one corresponds to the coagulation step ($t < 90$ s) where the paddle rotation speed is high.

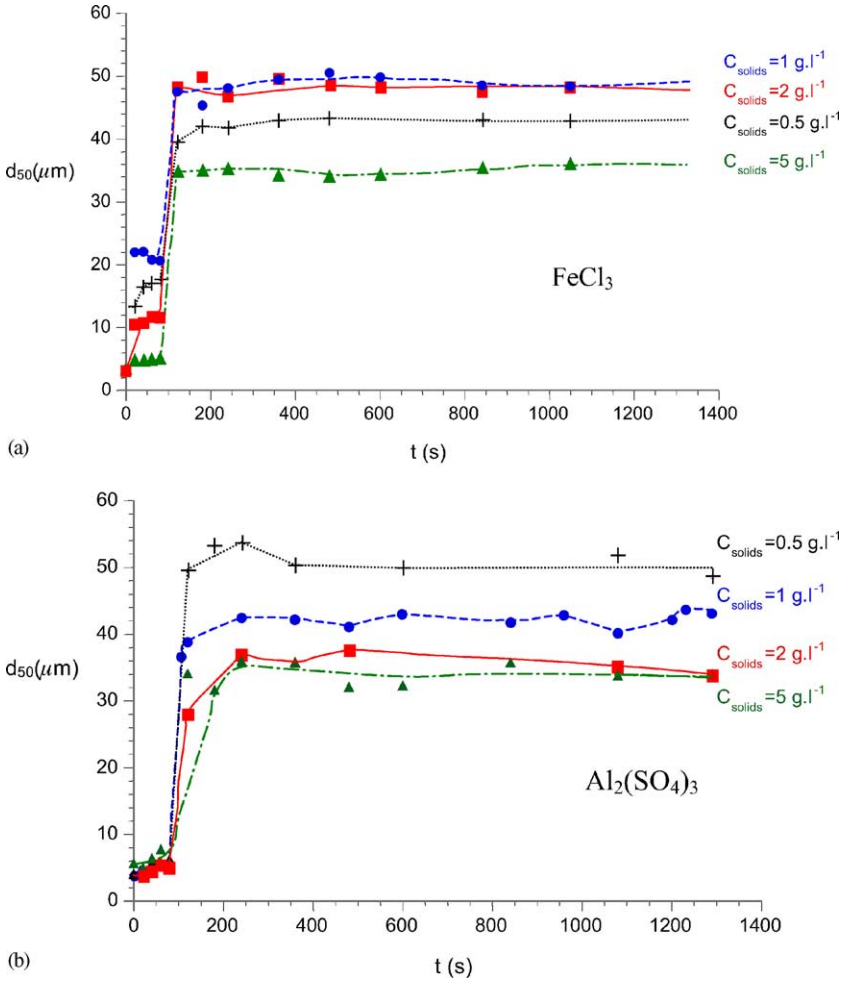

Fig. 4. Evolution of the median volume diameter d_{50} measured during coagulation: (a) for coagulation with $FeCl_3$; (b) for coagulation with $Al_2(SO_4)_3$.

During this first step, values of d_{50} are relatively low and slightly increase from 4 μm (initial clay particles diameter) to values comprised between 5 and 21 μm. After the flocculant addition ($t = 90$ s), d_{50} increases rapidly up to values comprised between 32 and 50 μm and remains almost constant despite the lowering of the paddle rotation speed at $t = 270$ s. This evolution is in agreement with the decomposition of the floc structure given in Fig. 1: the first part of the curve would correspond to the clustering (level 1) of the initial clay particles due to the action of the coagulant and the second one to the aggregation (level 2) of these clusters under the action of the flocculant. Although no more size evolution is observed, aggregates are supposed to group into large flocs (level 3) when the paddle rotation speed is lowered at $t = 270$ s. But these flocs are broken during the size analysis using the laser diffraction apparatus. Diameters of the different basic units are summarised in Table 2. The flocs apparent diameters D_{app} were obtained from image analysis during free settling tests. This two size measurement methods are known to give different results, comparison of the flocs diameters given here to those of clusters or aggregates would therefore be subjected to some error.

Whatever the coagulant used, the size increase observed after its adding is low compared to that observed after the

Table 2
Clusters and aggregates median volume diameters obtained from the curves in Fig. 3 (Malvern-Microsizer stirrer rotation speed = 1000 rpm) and flocs apparent median volume diameters obtained from image analysis during free settling tests (averaged on about 300 images)

C_{solids} (g L^{-1})	$FeCl_3$			$Al_2(SO_4)_3 \cdot 14H_2O$		
	$d_{50}^{clusters}$ (μm)	$d_{50}^{aggregates}$ (μm)	D_{app}^{flocs} (μm)	$d_{50}^{clusters}$ (μm)	$d_{50}^{aggregates}$ (μm)	D_{app}^{flocs} (μm)
0.5	16	42	888	4	50	1160
1	21	49	848	5	42	857
2	11	48	762	5	36	733
5	5	35	516	6	32	634

flocculant addition. This is due to the weakness of the bounds created between solids particles in the case of coagulation: as seen before, coagulation is solely due to the enmeshment of particles within hydroxide precipitates. Under high shear strains only small units can be formed. Flocculation is due to the entrapment of solids units by long polymer chains made of large molecules and exhibiting greater mechanical resistance. However, whilst aggregates and flocs sizes are similar for a given clay concentration, clusters are larger in ferric flocs than in alum ones. And, as a general rule, the basic units size decreases when C_{solids} is increased. It can be attributed to the higher number of collision occurring in more concentrated suspensions and causing structural reorganisations and compaction of the structure with expulsion of some of the free water entrapped.

Fig. 5 shows two examples for the log–log plots of u_l versus D_{app}. For each floc family, the volume fractal dimension D_3 given in Table 3 is calculated from the slope value of the linear regression obtained and Eq. (4). Considering the low accuracy on the D_3 values obtained, no clear variation of D_3 with the clay concentration appears. However, values obtained are high, about 2.5, meaning that the flocs studied here have rather compact structures. Coagulation was performed under ionic strengths lying between 10^{-3} and 4×10^{-3} M corresponding to RLA conditions [16] that usually lead to D_3 values about 2.1 [17]. Values as high as 2.5 shall be explained by an additional restructuring of the flocs. Actually, high shear environments were shown to lead to compaction, involving fragmentation and reformation of the floc and/or bending and twisting inside the floc [17,18]. For nickel hydrocarbonate particles aggregated under velocity gradient of 200 s^{-1}, Hoekstra [17] obtained a D_3 value of 2.7. The rotation speed of 200 rpm used in our experiments during the coagulation step (beakers without baffles, equipped with two-blade paddle impellers) would correspond to a rather high velocity gradient of about 120 s^{-1} [19]. The value of $D_3 \sim 2.5$ is therefore consistent with the results obtained by Hoekstra [17] and the restructuring theory. D_3 values obtained for aluminium and ferric flocs are close to each other, but those obtained for ferric flocs are always lower meaning that these flocs have a little more open structure than aluminium ones. This is in agreement with the average density values given in Table 3: even if close to each other whatever the coagulant used, they are always smaller for ferric flocs. Concerning the density increase observed when C_{solids} is increased it has been shown [10] that it is solely due to the corresponding decrease in the floc size since fractal entities with same D_3 are characterised by increasing densities and therefore increasing settling rates when the size decreases.

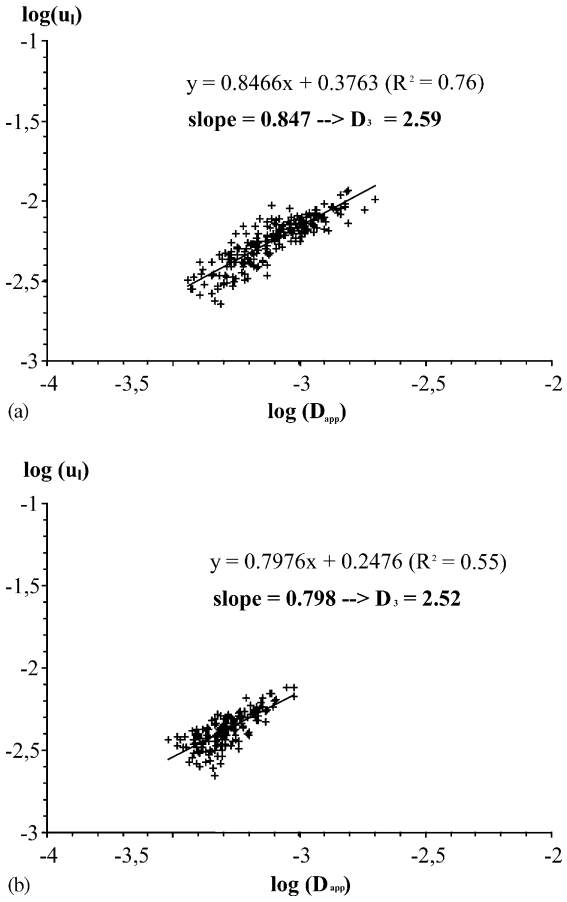

Fig. 5. Determination of the fractal dimension D_3 of clay flocs coagulated with aluminium sulphate, from the log–log plot of their settling velocity u_l (m s^{-1}) vs. their diameter D_{app} (m). (a) Clay concentration = 0.5 g L^{-1}; (b) clay concentration = 5 g L^{-1}.

3.2. Sludge dewaterability

The bound water content (W_{bound}) and the capillary suction time measured for the eight sludge families studied as well as for the initial clay suspension are given in Table 4. W_{bound} of the initial suspension is smaller than for coagulated clay. This can be easily understood considering the nature of flocs made of solids particles enmeshed

Table 3
Fractal dimension D_3 and average floc density ρ_{floc} obtained from Eq. (2) (with standard deviation)

C_{solids} (g L^{-1})	$FeCl_3$		$Al_2(SO_4)_3 \cdot 14H_2O$	
	D_3	ρ_{floc} (kg m^{-3})	D_3	ρ_{floc} (kg m^{-3})
0.5	2.44 (12%)	1030 (21%)	2.59 (8%)	1044 (10%)
1	2.48 (8%)	1051 (13%)	2.50 (8%)	1056 (14%)
2	2.47 (12%)	1055 (40%)	2.46 (8%)	1062 (14%)
5	2.45 (16%)	1056 (55%)	2.52 (16%)	1063 (77%)

Table 4
Bound water content and capillary suction time for the initial clay suspension and the eight sludges studied

C_{solids} (g L^{-1})	$FeCl_3$		$Al_2(SO_4)_3{\cdot}14H_2O$	
	W_{bound} (g/g dry solids)	CST (s)	W_{bound} (g/g dry solids)	CST (s)
Initial	0.12	176	0.12	176
0.5	0.39	98.1	0.41	67
1	0.22	85.5	0.32	59.8
2	0.23	75.7	0.25	61
5	0.20	75.7	0.25	55.5

within hydroxide precipitates and polymer chains with water adsorbed and entrapped during the floc growth. Coagulation–flocculation, therefore reduces the extent of dewatering, but it also greatly increases the rate of dewatering as shown by the greatly smaller CST values obtained for coagulated particles. Because dewatering resistance is related to surface drag losses, the shift to larger units in coagulated sludges reduces the specific surface area in the sludge matrix, yielding improved dewatering rates.

Concerning the influence of the coagulant used, it appears that the bound water contents are close for both ferric and alum sludges, but they are on average about 20% higher in this last case indicating a significantly lower extent of dewatering. At the same time, CST values are about 27% lower indicating a higher dewatering rate than for iron sludges. As shown in Fig. 6, in both cases CST value linearly decreases with the bound water content. A decrease in the bound water content has therefore also a positive effect on the resistance to filtration. A general correlation between CST and W_{bound} can be deduced

$$CST \cong 53 W_{bound} + B' \quad (5)$$

where B' is a constant depending on the coagulant used: $B' \cong 70$ s for $FeCl_3$ and $B' \cong 45$ s for $Al_2(SO_4)_3{\cdot}14H_2O$.

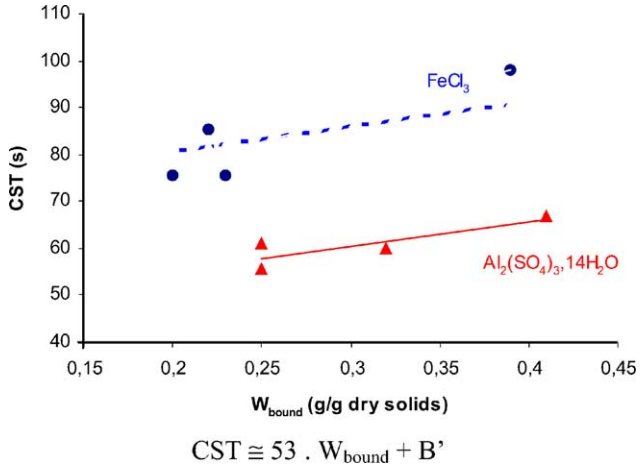

Fig. 6. Relation between bound water content and capillary suction time of clay sludges ($B' \cong 70$ s for $FeCl_3$ and $B' \cong 45$ s for $Al_2(SO_4)_3{\cdot}14H_2O$).

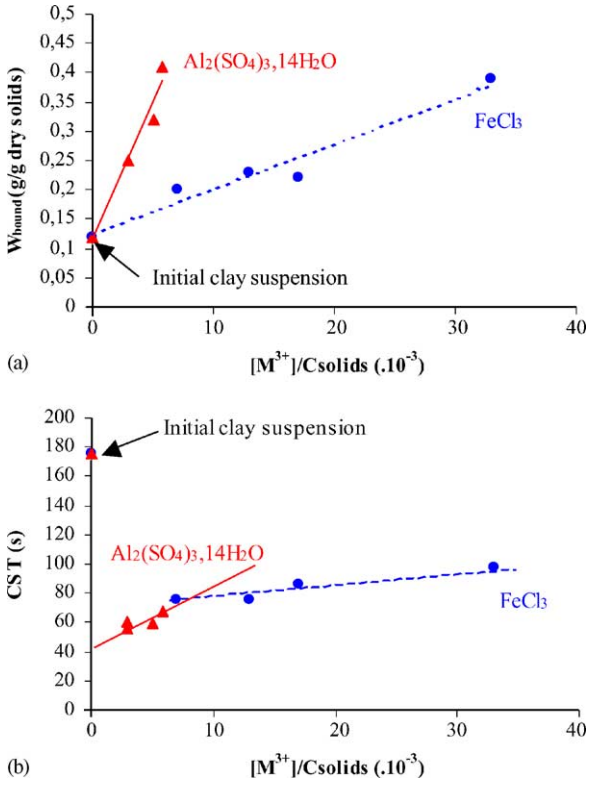

Fig. 7. Evolutions of the bound water content (a) and CST (b) vs. $[M^{3+}]/C_{solids}$.

Whatever the coagulant used, the solids concentration of the initial clay suspension appears to have a significant influence on the sludge dewaterability since both W_{bound} and CST decrease when C_{solids} increases. However, since the metal ion concentration $[M^{3+}]$ is varied for the different conditions tested, it seems more appropriate to follow the evolutions of W_{bound} and CST as a function of the ratio $[M^{3+}]/C_{solids}$ as proposed by Knocke et al. [2]. From the curves given in Fig. 7, it appears that whatever the coagulant, W_{bound} and CST are directly proportional to this ratio. Anyway, whilst W_{bound} is always lower and increases more slowly with $[M^{3+}]/C_{solids}$ for ferric sludges than for alum ones, CST is lower for the alum sludges considered here than for the ferric ones. These lower CST values may be due to the fact that the optimisation tests performed to determine the amounts of coagulant and flocculant (Table 1) have led to lower values of $[M^{3+}]$ for alum sludges. And, considering the points in Fig. 7(b) independently of the coagulant used, it appears that CST only depends on $[M^{3+}]/C_{solids}$ and will always be lower when this ratio is lower. The difference in bound water content can be related to the chemical characteristics of aluminium and iron. Actually, whilst Al^{3+} has an electrovalent character corresponding to a great preference for binding to water, Fe^{3+} is considered as a transition metal cation favouring binding to water to a lesser degree than does aluminium [20].

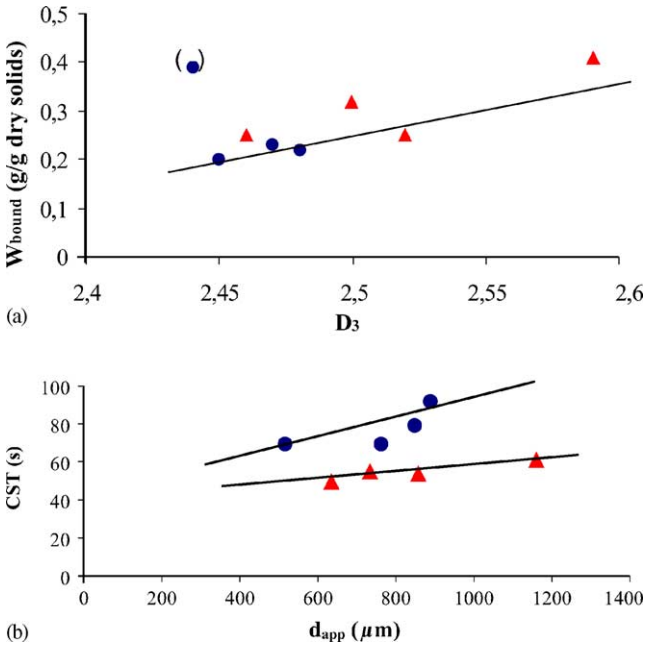

Fig. 8. Relation between floc structure and sludge dewaterability (●) $FeCl_3$, (▲) $Al_2(SO_4)_3$. $14H_2O$.

3.3. Relation between floc structure and sludge dewaterability

The floc families studied here were obtained by the same coagulation mechanism (sweep coagulation) and therefore exhibit very close structures. However, ferric flocs were found to have a little more open structure (lower D_3 values) than alum ones. They contain more water but smaller amounts of bound water. This relation between the fractal dimension D_3 and the bound water content of the corresponding sludge is confirmed besides by the curve in Fig. 8(a) where, except for one point, the bound water content decreases when the fractal dimension decreases. A lower compactness of the flocs is therefore indicative of a higher extent of the sludge dewaterability since a lower part of the water is bound to the solid. The slightly smaller D_3 values obtained for ferric flocs (about 1%) are therefore very significant for sludge dewaterability since they lead to a decrease of bound water of about 12% compared to alum sludges.

The sludge resistance to water withdrawal is also related to the floc structure. Actually, the curve in Fig. 8(b) shows that, at the opposite of one could have expected considering surface drag losses, the capillary suction time is lower when flocs are smaller. And, for the same apparent floc diameter, CST is lower for alum flocs where clusters were found smaller.

4. Conclusions

Eight synthetic clay flocs families were produced by sweep coagulation using clay suspensions with different initial concentrations and two coagulants in common use. Particle size analysis performed during coagulation showed that these flocs were made of three basic units (clusters, aggregates and flocs).

The flocs structure was characterised by the size of these units and by the floc fractal dimension D_3. All the eight families exhibited rather compact structures ($D_3 \approx 2.5$) and the flocs as well as aggregates and clusters sizes decreased when the initial solids concentration was increased. Ferric flocs were found to be slightly smaller and less compact than alum ones they are therefore expected to settle badly.

The dewaterability of sludges produced from these different flocs was characterised measuring the bound water content and the capillary suction time indicative, respectively, of the possible extent and of the rate of water removal during dewatering. Significant differences were observed between ferric and alum sludges and as a function of the initial clay suspension concentration. Due to the electrovalent character of Al^{3+}, more water was bound in alum sludges. These sludges therefore could not be dewatered as far as ferric ones. But, at the same time, in the case of coagulation with $Al_2(SO_4)_3$, the optimisation of the coagulation conditions had led to lower concentrations in metallic ion $[M^{3+}]$ and to lower capillary suction times since it was shown that CST decreased with the ratio $[M^{3+}]/C_{solids}$. Alum sludges could therefore be dewatered more rapidly than ferric ones.

Rules in the choice of the coagulant and in the required solids concentration during coagulation can be deduced from this study:

1. Higher solids concentration leads to smaller flocs with smaller basic units and to sludges containing less bound water with low CST. These sludges are therefore dewatered farer and faster than those obtained with low solids concentrations.
2. Alum flocs are larger and more compact than ferric ones, they settle faster and lead to sludges containing about 20% more bound water but having lower resistance to water removal.

References

[1] Y.Q. Zhao, Correlations between floc physical properties and optimum polymer dosage in alum sludge conditioning and dewatering, Chem. Eng. J. 92 (2003) 227–235.
[2] W.R. Knocke, J.R. Hamon, B.E. Dulin, Effects of coagulation on sludge thickening and dewatering, J. AWWA 86 (6) (1987) 89–98.
[3] C.C. Wu, J.J. Wu, R.Y. Huang, Floc strength and dewatering efficiency of alum sludge, Adv. Environ. Res. 7 (2003) 617–621.
[4] J.Y. Bottero, B. Lartiges, Séparation liquide/solide par coagulation–floculation: les coagulants–floculants, mécanismes d'agrégation, structure et densité des flocs, Bull. Sci. Géol. 46 (1–4) (1993) 163–174.
[5] J. Namer, J.J. Ganczarczyk, Settling properties of digested sludge particle aggregates, Water Res. 27 (8) (1993) 1285–1294.
[6] D. Snidaro, F. Zartarian, F. Jorand, J.Y. Bottero, J.C. Block, J. Manem, Characterization of activated sludge flocs structure, Water Sci. Technol. 36 (4) (1997) 313–320.

[7] B.B. Mandelbrot, The Fractal Geometry of Nature, Freeman, San Francisco, CA, 1982.
[8] M. Smollen, Evaluation of municipal sludge drying and dewatering with respect to sludge volume reduction, Water Sci. Technol. 22 (12) (1990) 153–161.
[9] P.A. Vesilind, C.J. Martel, Freezing of water and wastewater sludges, J. Environ. Eng.—ASCE 116 (1990) 854–862.
[10] C. Fargues, C. Turchiuli, Structural characterisation of flocs in relation to their settling performances, Chem. Eng. Res. Des. 81 (9) (2003) 1171–1178.
[11] P.N. Johnson, A. Amirtharajah, Ferric chloride and alum as single and dual coagulants, J. AWWA 75 (5) (1983) 232–239.
[12] C.P. Johnson, X. Li, B.E. Logan, Settling velocities of fractal aggregates, Environ. Sci. Technol. 30 (6) (1996) 1911–1918.
[13] H. Wadell, The coefficient of resistance as a function of Reynold's number for solids of various shape, J. Franklin Inst. 217 (1934) 459–490.
[14] Y. Adachi, Y. Tanaka, Settling velocity of an aluminium–kaolinite floc, Water Res. 31 (3) (1997) 449–454.
[15] H. Heukelekian, E. Weisberg, Bound water and activated sludge bulking, Sewage Ind. Wastes 28 (4) (1956) 558–574.
[16] M.Y. Lin, H.M. Lindsay, D.H. Weitz, R.C. Ball, R. Klein, P. Meakin, Universality in colloid aggregation, Nature 339 (1989) 360–362.
[17] L.L. Hoekstra, R. Vreeker, W.G.M. Agterof, Aggregation of colloidal nickel hydroxycarbonate studied by light scattering, J. Colloid Interf. Sci. 151 (1) (1992) 17–25.
[18] K.A. Kusters, J.G. Wijers, D. Thoenes, Aggregation kinetics of small particles in agitated vessels, Chem. Eng. Sci. 52 (1) (1997) 107–121.
[19] R.J. Lai, H.E. Hudson Jr., J.E. Singley, Velocity gradient calibration of jar-test equipment, J. Am. Water Works Assoc. 67 (1975) 553–557.
[20] W. Stumm, J.J. Morgan, Aquatic Water Chemistry, Wiley, New York, 1981.